ANNALS of Faculty Engineering Hunedoara
– International Journal of Engineering
Tome XIV [2016] – Fascicule 2 [May]
ISSN: 1584-2665 [print; online]
ISSN: 1584-2673 [CD-Rom; online]
a free-accessmultidisciplinarypublication
of theFaculty of Engineering Hunedoara

[1.]Dilruba YASMIN, [2.]Tanvir AHMED, [3.]Nisat Nowroz ANIKA,
[4.]Mohammad FERDOWS,[5.]Md. Mahmud ALAM

VISCO-ELASTIC FLUID FLOW ON MHD FREE CONVECTION AND MASS TRANSFER FLOW WITH THERMAL AND MASS DIFFUSION

[1-3, 5.]Mathematics Discipline, Khulna University, Khulna, BANGLADESH
[4.] Department of Applied Mathematics, University of Dhaka, Dhaka, BANGLADESH

ABSTACT: MHD heat and mass transfer viscoelastic fluid flow through a vertical porous plate with Dufour and Soret effect has been studied. In this analysis, the viscoelastic fluid in the momentum equation is considered for high speed fluid flows and the level of concentration have been taken very high. The governing equations of the problem contain a system of partial differential equations. Usual nondimensional variables have been used to obtain the dimensionless momentum, energy and concentration equations. The dimensionless coupled partial differential equations are solved numerically by implicit finite difference method. The simulated results of this investigation are discussed for the different values of the well-known parameters with different time steps. Finally, the obtained numerical results are compared with previous published results and this comparison has been shown in tabular form.
Keywords: MHD, visco-elastic fluid, Dufour effect, Soret effect

1. INTRODUCTION

Many common liquids such as oils, certain paints, polymer solution, some organic liquids and many new material of industrial importance exhibit both viscous and elastic properties. Therefore, the above fluids called viscoelastic fluids .The research on visco-elastic fluids is gaining a lot of attention in recent year. The study of Magneto hydrodynamics (MHD) boundary layer flow of a visco-elastic fluid flow through vertical porous plate in the presence of thermal diffusion and mass diffusion have become the basic of several industrial, science and engineering applications. The mixed convection boundary layer flow of non-Newtonian fluid in the presence of magnetic field has wide range of application in nuclear engineering and industries. In astrophysical and geophysical studies, the MHD boundary layer flows of an electrically conducting fluid have also enormous applications. Many researchers have studied the transient laminar natural convection flow past a vertical porous plate for the application in the branch of science and technology such as in the field of agriculture engineering and chemical engineering. In petroleum refineries, movement of oil, water and gas through porous media for purification and filtration are bright applied areas of research. With the advancement of science and technology, MHD study on any fluid flow phenomenon exhibits some results which have constructive application for the design of devices. MHD heat transfer has great importance in the liquid metal flows, ionized gas flow in a nuclear reactor and electrolytes. Research works on radiation of heat in natural convection flow are very limited, though these have many modern applications viz. missile technology used in army, nuclear power plant, parts of aircraft and ceramic tiles. Heat and mass transfer in non-Newtonian fluids is of great interest in many operations in the chemical and process engineering industries including coaxial mixers, blood

oxygenators, milk processing, steady-state tubular reactors, and capillary column inverse gas chromatography devices, mixing mechanisms, bubble-drop formation processes, dissolution processes, and cloud transport phenomena. Many geometrical configurations have been addressed including flat plates, channels, cones, spheres, wedges, inclined planes, and wavy surfaces. Viscoelastic properties can enhance or depress heat transfer rates, depending upon the kinematic characteristics of the flow field under consideration and the direction of heat transfer. The viscous force imparted by a flowing fluid in a dense swarm of particles has been investigated by Brinkman (1947). The mass transfer effects on unsteady flow past an accelerated vertical porous plate have been discussed by Das et al. (2006). For such a fluid considering the oscillatory two-dimensional viscoelastic flow along an infinite porous wall, showing that an increase in the Walters elasticity parameter and the frequency parameter reduces the phase of the skin-friction has been investigated by Soundalegkar and Puri (1969). The laminar flow of an electrical-conducting Walter's liquid, past an infinite non-conducting vertical plate for impulsive as well as uniformly accelerated motion of the plate has been presented by Samria et al. (1990), in the presence of a transverse magnetic field. The Unsteady magneto hydrodynamic flows in a rotating elasto-viscous fluid have been analyzed by Nanousis (1992).The MHD free convection flow of a visco-elastic fluid past a vertical porous plate has been investigated by Chowdhury and Islam (2000). Recently, the effects of thermal radiation on unsteady free convection flow of an elasto-viscous fluid over a moving vertical plate with variable temperature in the presence of magnetic field through porous medium have been studied be Rajesh and Varma (2011). The analytical study of Heat source and mass transfer effects on MHD free convection flow of a visco-elastic fluid past an exponentially accelerated infinite vertical plate with variable temperature through porous medium has been investigated by Rakesh Kumar et al. (2011). The heat and mass transfer occur simultaneously between the fluxes, the driving potentials are of more intricate nature. An energy flux can be generated not only by temperature gradients but by composition gradients. The energy flux caused by a composition is called Dufour or diffusion-thermo effect. Temperature gradients can also create mass fluxes, and this is the Soret or thermal-diffusion effect. Generally, the thermal-diffusion and the diffusion-thermo effects are of smaller-order magnitude than the effects prescribed by Fourier's or Fick's laws and are often neglected in heat and mass transfer processes. The thermal-diffusion effect, for instance, has been utilized for isotope separation and in mixture between gases with very light molecular weight (H_2, He) and of medium molecular weight (Nitrogen-air) the diffusion-thermo effect was found to be of a magnitude such that it cannot be neglected. Many transport processes can be found in various ways in both nature and technology, in which the combined heat and mass transfer occur due to buoyancy forces caused by thermal diffusion and mass diffusion. Some of the convective heat and mass transfer processes with phase change include the evaporation of liquid at the interface between a gas and liquid or the sublimation at a solid-gas interface. The process of mass transfer affects all separation processes in chemical engineering such as the drying of solid materials, distillation, extraction and absorption. Heat and mass transfer for Soret and Dufour effect on mixed convection boundary layer flow over a stretching vertical surface in a porous medium filled with a viscoelastic fluid has been analyzed by Hayat et al. (2010). The steady mixed convection boundary layer flow due to the combined effect of heat and mass transfer over a stretched vertical surface in a porous medium filled with a viscoelastic fluid under Soret and Dufour effects in the presence of magnetic field has been investigated by Gbadeyan et al. (2011). Mixed convective MHD flow of visco-elastic fluid past a vertical infinite plate with mass transfer in the presence of magnetic field has been studied by Mahanta and Choudhury (2012)and containing governing equations have been solved analytically.

The objective of this study is to extend the work of Mahanta and Choudhury (2012) with visco-elastic fluid flow. It is characterized by second-order fluid as MHD free convection and mass transfer visco-elastic fluid flow in vertical porous plate with mass diffusion and thermal diffusion. The problem has been solved by implicit finite difference method. The governing equations involved in this problem have been transformed into non-similar coupled partial differential equations by usual transformations. The results of this study will be discussed for the different values of the well-known parameters and will be shown graphically.

2. MATHEMATICAL MODEL OF THE FLOW

An unsteady MHD visco-elastic mixed convective heat and mass transfer flow of an incompressible, electrically conducting viscous fluid past an electrically nonconducting

isothermal impulsive vertical infinite plate is considered. The positive x coordinate is measured along the plate in the direction of fluid motion and the positive y coordinate is measured normal to the plate. A uniform magnetic field of magnitude B_0 is applied in the direction of $y-\text{axis}$. Initially, it is considered that the plate as well as the fluid is at the same temperature $T(=T_\infty)$ and concentration level $C(=C_\infty)$. Also it is assumed that the temperature of the plate and spices concentration are raised to $T_w(>T_\infty)$ and $C_w(>C_\infty)$ respectively, which are there after maintained constant, where T_w, C_w are temperature and spices concentration at the wall and T_∞, C_∞ are the temperature and concentration of the species outside the boundary layer respectively. Since the plate is of infinite extent and the fluid motion is unsteady, so all the flow will depend only upon y and t. The physical configuration of the problem is furnished in Figure1.

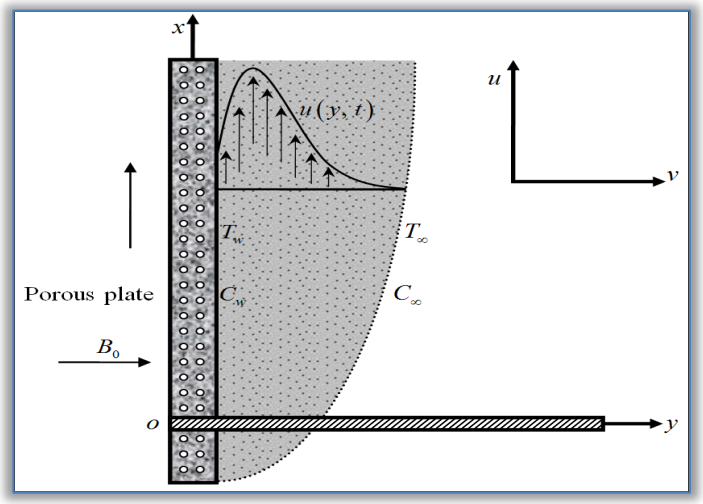

Figure1.Physical configuration and coordinate system

The physical model of this study is furnished in the following figure.

The generalized equations relevant to the unsteady problem are governed by the following system of coupled partial differential equations as:

$$\frac{\partial v}{\partial y}=0 \tag{1}$$

The Momentum equation:

$$\frac{\partial u}{\partial t}-v_0\frac{\partial u}{\partial y}=g\beta\left(T-T_\infty\right)+g\beta^*(C-C_\infty)+\upsilon_1\left(\frac{\partial^2 u}{\partial y^2}\right)+\upsilon_2\left\{\frac{\partial^2}{\partial y^2}\left(\frac{\partial u}{\partial t}\right)+v\frac{\partial^3 u}{\partial y^3}\right\}-\frac{\sigma B_0^2 u}{\rho} \tag{2}$$

The Energy equation:

$$\frac{\partial T}{\partial t}-v_0\frac{\partial T}{\partial y}=\frac{\kappa}{\rho C_p}\frac{\partial^2 T}{\partial y^2}+\frac{D\kappa_t}{C_pC_s}\frac{\partial^2 T}{\partial y^2} \tag{3}$$

The Concentration equation:

$$\frac{\partial C}{\partial t}-v_0\frac{\partial C}{\partial y}=D\frac{\partial^2 C}{\partial y^2}+\frac{D\kappa_t}{T_m}\frac{\partial^2 T}{\partial y^2} \tag{4}$$

The corresponding boundary conditions for the problem are

$$\begin{aligned} u=U_0, \quad & T=T_w, && C=C_w \quad \text{at } y=0 \\ u=0, \quad & T\to T_\infty, && C\to C_\infty \quad \text{as } y\to\infty \end{aligned} \tag{5}$$

where g is the local acceleration due to gravity; β is the thermal expansion coefficient; β^* is the concentration expansion coefficient; υ_1, υ_2 are the kinematic viscosities; ρ is the density of the fluid; B_0 is the constant induced magnetic field; σ is the electrical conductivity; κ is the thermal conductivity; c_p is the specific heat at the constant pressure; c_s is the concentration susceptibility; D is the coefficient of mass diffusivity; κ_t is the thermal diffusion ratio and T is the mean fluid temperature at the wall.

3. MATHEMATICAL FORMULATION

Since the solutions of the governing equations (2)-(4) under the boundary conditions (5) will be based on the finite difference method, so it is required to make the equations dimensionless. The following non-dimensional quantities are introduced:

$$Y=\frac{yU_0}{\upsilon_1}, \bar{U}=\frac{u}{U_0}, \tau=\frac{tU_0^2}{\upsilon_1}, \bar{\theta}=\frac{T-T_\infty}{T_w-T_\infty} \text{ and } \bar{\varphi}=\frac{C-C_\infty}{C_w-C_\infty}.$$

Substituting the above dimensionless variables in equations (2)-(4), the following nonlinear coupled partial differential equations have been obtained.

$$\frac{\partial \bar{U}}{\partial \tau} - S\frac{\partial \bar{U}}{\partial Y} = \frac{\partial^2 \bar{U}}{\partial Y^2} + G_r\bar{\theta} + G_m\bar{\varphi} + \alpha\left[\frac{\partial^2}{\partial Y^2}\left(\frac{\partial \bar{U}}{\partial \tau}\right) - S\frac{\partial^3 \bar{U}}{\partial Y^3}\right] - M_{ha}\bar{U} \tag{6}$$

$$\frac{\partial \bar{\theta}}{\partial \tau} - S\frac{\partial \bar{\theta}}{\partial Y} = \frac{1}{P_r}\frac{\partial^2 \bar{\theta}}{\partial Y^2} + D_u\frac{\partial^2 \bar{\varphi}}{\partial Y^2} \tag{7}$$

$$\frac{\partial \bar{\varphi}}{\partial \tau} - S\frac{\partial \bar{\varphi}}{\partial Y} = \frac{1}{S_c}\frac{\partial^2 \bar{\varphi}}{\partial Y^2} + S_r\frac{\partial^2 \bar{\theta}}{\partial Y^2} \tag{8}$$

The corresponding boundary conditions for the problem are given below.

$$\begin{aligned} &\bar{U} = 1, && \bar{\theta} = 1, && \bar{\varphi} = 1 && \text{at } Y = 0 \\ &\bar{U} = 0, && \bar{\theta} = 0, && \bar{\varphi} = 0 && \text{as } Y \to \infty \end{aligned} \tag{9}$$

where, Grashof number for Heat transfer, $G_r = \frac{g\beta(T_w - T_\infty)\upsilon_1}{U_0^3}$, Grashof numberfor Mass transfer, $G_m = \frac{g\beta^*(C_w - C_\infty)\upsilon_1}{U_0^3}$, Hartmann number, $M_{ha} = \frac{\sigma B_0^2 U_0 \upsilon_1}{\rho U_0^3}$, Visco-elastic parameter, $\alpha = \frac{\upsilon_2}{\upsilon_1^2}U_0^2$, Prandtl number, $P_r = \frac{\upsilon_1}{\kappa}$, Duffour number, $D_u = \frac{D\kappa_t}{C_s C_p}\frac{(C_w - C_\infty)}{\upsilon_1(T_w - T_\infty)}$, Schmidt number $S_c = \frac{\upsilon_1}{D}$, Sorret number, $S_r = \frac{D\kappa_t}{\upsilon_1}\frac{(T_w - T_\infty)}{(C_w - C_\infty)}$, Suction number $S = \frac{v_0}{U_0}$.

4. SHEAR STRESS, NUSSELT NUMBER AND SHERWOOD NUMBER

The quantities of chief physical interest are shear stress, Nusselt number and Sherwood number. From the velocity field, the effects of various parameters on the plate shear stress have been calculated. The following equation represents shear stress at the plate:

Shear stress, $\tau_x = \mu_0\left(\frac{\partial \bar{U}}{\partial Y}\right)_{Y=0}$

From the temperature field, the effects of various parameters on the heat transfer coefficients have been analyzed. The following equation represents the well-known Nusselt number.

Nusselt number, $N_u = \mu_0\left(-\frac{\partial \bar{\theta}}{\partial Y}\right)_{Y=0}$

From the concentration field, the effects of various parameters on the mass transfer coefficients have been analyzed. The following equation represents the well-known Sherwood number.

Sherwood number, $S_h = \mu_0\left(-\frac{\partial \bar{\varphi}}{\partial Y}\right)_{Y=0}$.

5. NUMERICAL SOLUTIONS

For simplicity, the implicit finite difference method has been used to solve equations (1)-(3) subject to the boundary conditions has been given by (5). To obtain the difference equations the region of the flow is divided into a grid or mesh of lines parallel to X and Y axes where X-axis is taken along the plate and Y-axis is normal to the plate.

Here it is assumed that the maximum length of boundary layer is $Y_{\max}(=35)$ as corresponds to $Y \to \infty$. That is Y varies from 0 to 35 and the number of grade

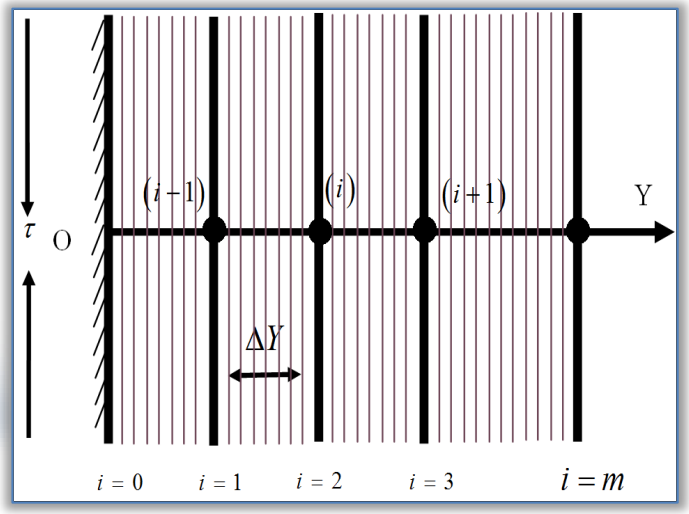

Figure 2. Implicit Finite difference space grid

spacing in Y direction is $m=180$. The constant mesh size along Y axis becomes $\Delta Y=0.17\left(0\le y\le 35\right)$ with a smaller time step $\Delta\tau=0.005$ and grid spacing's in Y direction is has been show in Figure2.

The corresponding differential equations are obtained an appropriate set of finite difference equations;

$$\frac{\bar{U}_i^{n+1}-\bar{U}_i^n}{\Delta\tau}-S\frac{\bar{U}_{i+1}^n-\bar{U}_i^n}{\Delta Y}=G_r\bar{\theta}_i^n+G_m\bar{\varphi}_i^n+\frac{\bar{U}_{i+1}^n-2\bar{U}_i^n+\bar{U}_{i-1}^n}{\left(\Delta Y\right)^2}-M_{ha}\bar{U}_i^n+\alpha\left[\frac{\bar{U}_{i+1}^{n+1}-2\bar{U}_i^{n+1}+\bar{U}_i^{n+1}-\bar{U}_{i+1}^n+2\bar{U}_i^n-\bar{U}_{i-1}^n}{\Delta\tau\left(\Delta Y\right)^2}\right]$$

$$-\alpha S\left[\frac{\bar{U}_{i+2}^n-2\bar{U}_{i+1}^n+2\bar{U}_{i-1}^n-\bar{U}_{i-2}^n}{2\left(\Delta Y\right)^3}\right] \tag{10}$$

$$\frac{\bar{\theta}_i^{n+1}-\bar{\theta}_i^n}{\Delta\tau}-S\frac{\bar{\theta}_{i+1}^n-\bar{\theta}_i^n}{\Delta Y}=\frac{1}{P_r}\frac{\bar{\theta}_{i+1}^n-2\bar{\theta}_i^n+\bar{\theta}_{i-1}^n}{\left(\Delta Y\right)^2}+D_u\frac{\bar{\varphi}_{i+1}^n-2\bar{\varphi}_i^n+\bar{\varphi}_{i-1}^n}{\left(\Delta Y\right)^2} \tag{11}$$

$$\frac{\bar{\varphi}_i^{n+1}-\bar{\varphi}_i^n}{\Delta\tau}-S\frac{\bar{\varphi}_{i+1}^n-\bar{\varphi}_i^n}{\Delta Y}=\frac{1}{S_c}\frac{\bar{\varphi}_{i+1}^n-2\bar{\varphi}_i^n+\bar{\varphi}_{i-1}^n}{\left(\Delta Y\right)^2}+S_r\frac{\bar{\theta}_{i+1}^n-2\bar{\theta}_i^n+\bar{\theta}_{i-1}^n}{\left(\Delta Y\right)^2} \tag{12}$$

The boundary conditions with the finite difference scheme are

$$\bar{U}_0^n=1,\qquad \theta_0^n=1,\qquad \varphi_0^n=1$$

$$\bar{U}_L^n=1,\qquad \theta_L^n=1,\qquad \varphi_L^n=1\text{ where }L\to\infty. \tag{13}$$

The subscripts i designate the grid points with Y coordinate and the superscript n represents a value of time, $\tau=n\Delta\tau$ where $n=0,\,1,\,2,\ldots.$ The velocity $\left(\bar{U}\right)$, temperature $\left(\bar{\theta}\right)$ and concentration $\left(\bar{\varphi}\right)$ distributions at all interior nodal points may be computed by successive applications of the above finite difference equations. The numerical values of the shear stress, Nusselt number and Sherwood number are evaluated by Five-point approximate formula for the derivatives. Since an implicit procedure is being used, the analysis will remain incomplete unless the stability analysis of the finite difference is performed. For the constant mesh size, the stability criteria of the scheme may be established. The stability conditions of the problem are $S\frac{\Delta\tau}{\Delta Y}+\frac{2}{P_r}\frac{\Delta\tau}{\left(\Delta Y\right)^2}\le 1$ and $S\frac{\Delta\tau}{\Delta Y}+\frac{2}{S_c}\frac{\Delta\tau}{\left(\Delta Y\right)^2}\le 1$.

6. RESULTS AND DISCUSSION

The numerical solutions are obtained for various parameters with small values of Dufour number. In order to analyze the physical situation of the model, the steady state numerical values of the non-dimensional velocity $\left(\bar{U}\right)$, temperature $\left(\bar{\theta}\right)$ and concentration $\left(\bar{\varphi}\right)$ within the boundary layer for different values of magnetic parameter $\left(M_{ha}\right)$, Soret number $\left(S_r\right)$, Prandtl number $\left(P_r\right)$, Grashof number $\left(G_r\right)$, Schmidt number $\left(S_c\right)$, Dufour number $\left(D_u\right)$, Visco-elastic parameter $\left(\alpha\right)$, Suction number $\left(S\right)$ and Modified Grashof number $\left(G_m\right)$ have been computed.

To get the implicit solutions, the computations have been carried out upto $\tau=80.05$. Because of the special importance of cooling problem in nuclear engineering in connection with the cooling of reactors, the value of the Grashof number for heat transfer is takentobepositive $\left(G_r>0\right)$.Since the most important fluids are atmospheric air, salt water and water so the results are limited to $P_r=0.71$ (Prandtl number for air at 20°C), $P_r=1.0$ (Prandtl number for salt water at 20°C)and $P_r=7.0,0.75$ (Prandtl number for water at 20°C). The investigation are assumed for both lighter and heavier fluid particles, hence with respect to the convergence criteria of the problem the values of Schmidt number $\left(S_c\right)$ are taken 0.60, 0.78 and 1.0 (in particular, 0.60 for water vapor that represents a diffusing chemical species of most common interest in air, 0.78 corresponds to ammonia and 1.0 for carbondioxide at 25°C temperature and 1 atmospheric pressure) which represent the specific condition of the flow. However the

values of another parameters M_{ha}, S_c, S_r, P_r, α and D_u are chosen arbitrarily and also the modified Grashof number $G_m = 1.0$ for mass transfer are considered as a fixed value.Along with the obtained the solutions, the flow behaviors in case of cooling problem are discussed graphically. The profiles of the velocity, temperature and species concentration versus Y are illustrated in Figures (3-17).The velocity profiles have been shown in Figures (3-11). The effect of the visco-elastic parameter(α)on the velocity field is presented in Figure 3 that$U$ decreases with the increase of visco-elastic parameter(α).

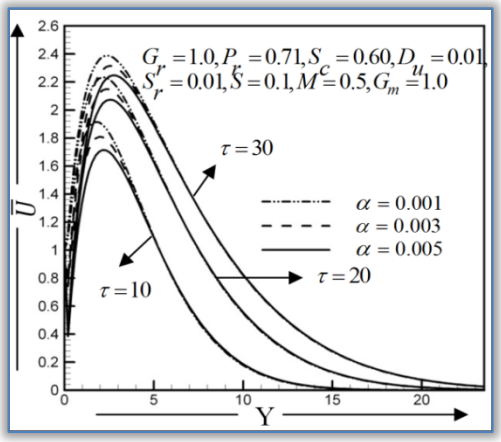

Figure 3. Velocity profiles U for differentvalues of visco-elastic parameter, α.

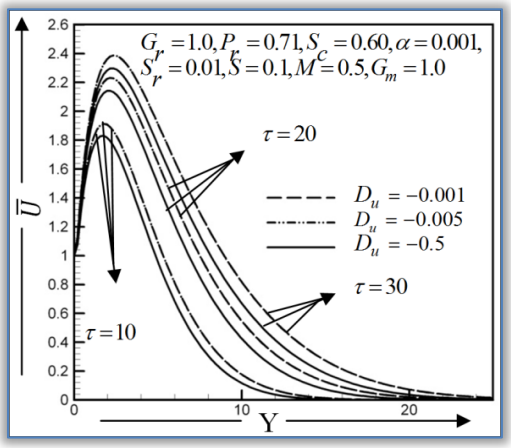

Figure 4. Velocity profiles $\bar{U}$ for different values of dufour number, D_u.

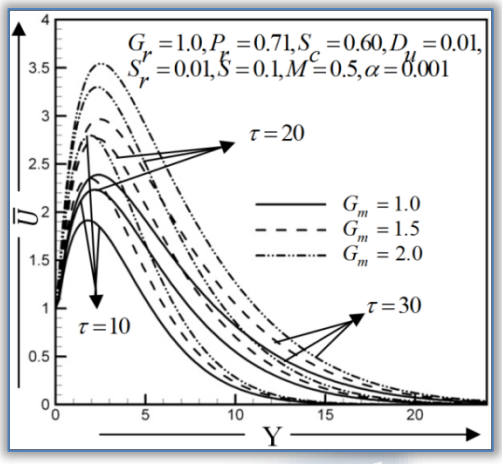

Figure 5. Velocity profiles $\bar{U}$ for different values of modified grashof number, G_m.

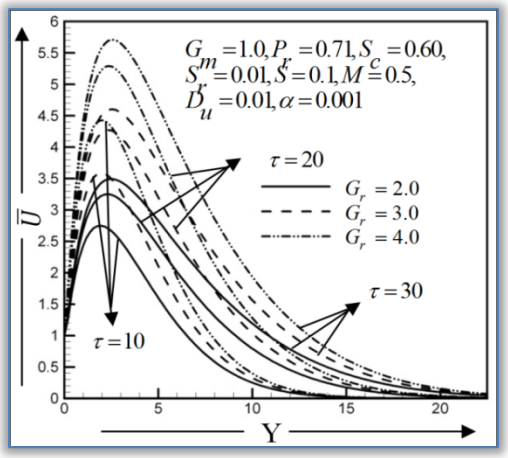

Figure 6. Velocity profiles $\bar{U}$ for different values of Grashof number, G_r.

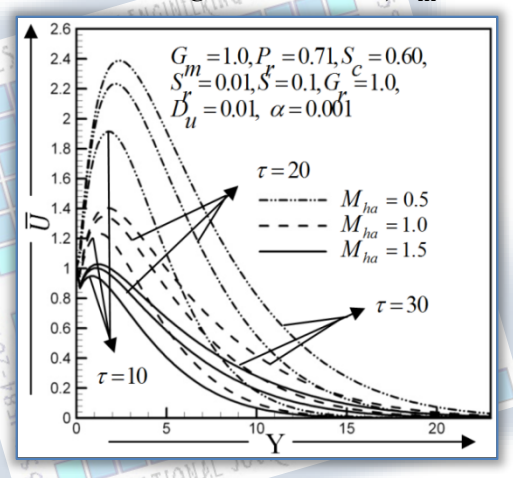

Figure 7. Velocity profiles $\bar{U}$ for different values of Hartmann numberer, M_{ha}.

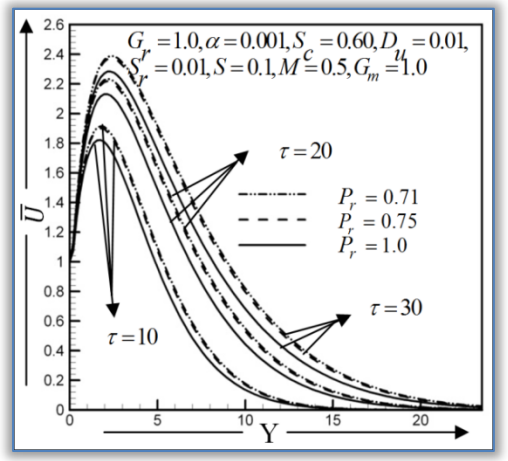

Figure 8. Velocity profiles $\bar{U}$ for different values of Prandtl number, P_r.

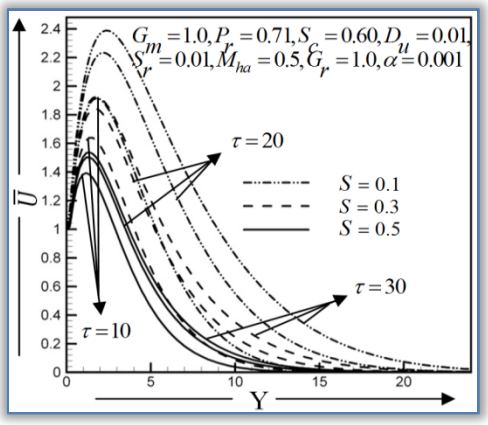

Figure 9. Velocity profiles $\bar{U}$ for different values of Suction number, S.

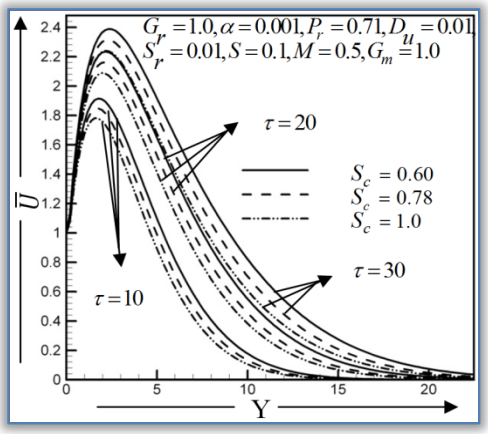

Figure 10. Velocity profiles $\bar{U}$ for different values of Schmidt number, S_c.

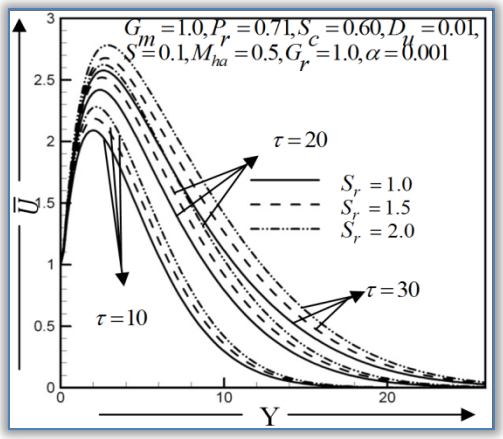

Figure 11. Velocity profiles $\bar{U}$ for different values of Soret number, S_r.

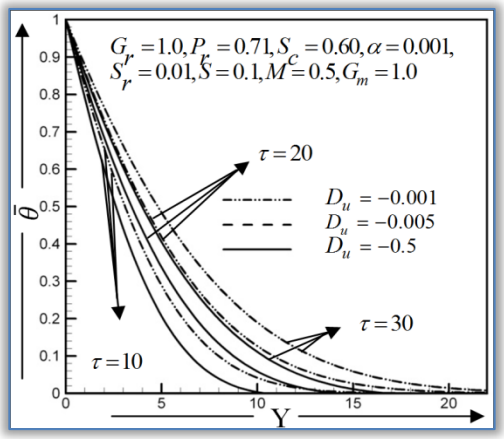

Figure 12. Temperature distributions $\bar{\theta}$ for different values of Dufour number, D_u.

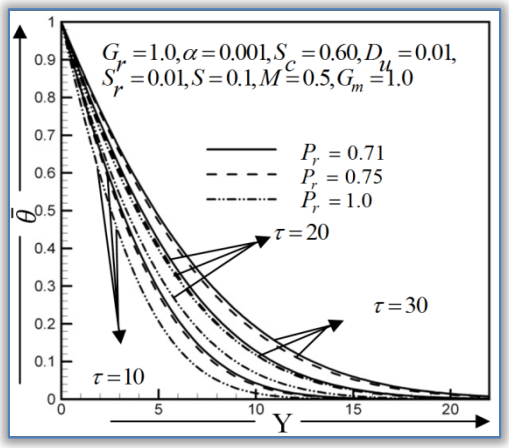

Figure 13. Temperature distributions $\bar{\theta}$ for different values of Prandtl number, P_r.

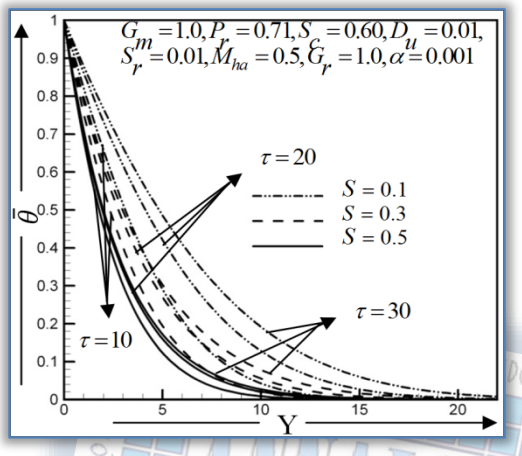

Figure 14. Temperature distributions $\bar{\theta}$ for different values of Suction number, S.

The effect of the Dufour number (D_u) on the velocity field is presented in Figure4. It is observed that the velocity decreases with the decrease the value of D_u. The velocity profiles (U) increases with the increase modified of Grashof number (G_m) in Figure 5. The effect of the Grashof number (G_r) on the velocity field is presented in Figure6. It is observed that the velocity profiles increases with the increase of G_r. For extremely cooled plate $(G_r > 0)$, the fluid velocity rapidly increases with the increase of G_r.The effect of the magnetic parameter Hartmann number (M_{ha}) on the velocity field is presented in Figure7. It is observed that the velocity

profiles decreases with the increase of M_{ha}. The effect of the Prandtl number(P_r)on the velocity field is presented in Figure 8. It is observed that the velocity decreases with the increases the value of P_r. The effect of the Suction number(S)on the velocity field is presented in Figure9. It is observed that the velocity decreases with the increase of S. The velocity profiles show that velocity decreases with the increase of S_c in Figure10. In particular, the velocity is larger for water vapor than carbondioxide. The effect of the Soret number(S_r)on the velocity field is presented in Figure 11. It is observed that the velocity increases with the increase the value of S_r. The velocity profiles show that velocity rises with the increase of S_r. Figures 12-14 represent the effects of the temperature profile for Dufour number, Prandtl number and Suction number. The temperature decreases with the decrease of Dufour number. The temperature distributions decreases with the increase of Prandtl number(P_r). The temperature decreases with increase of Suction number (S)For minor effect on$\bar{\theta}$, another graphical representation are not discussed. The effect of Suction number on concentration distributions is presented in Figure15. It is observer that concentration distributions decrease with the increase of Suction number(S). Figure 16 shows that concentration distributions decrease with the increase of Schmidt number(S_c). Physically, the increase of S_c means decrease of molecular diffusivity. The concentration of species is higher for small values of S_c and lower for large values of S_c. The concentration distributions increases with the increase of Soret number(S_r), which is shown in Figure 17 and it is observed that concentration distributions gradually increases with the increase of S_r. The behaviour of the quantities of chief physical interest as shear stress(τ_x), Nusselt number$(N_u)$and Sherwood number(S_h) for different values of visco-elastic parameter(α), Soret number(S_r), Hartmann number(M_{ha}), Modified Grashof number(G_m), Grashof number(G_r), Prandtl number(P_r), Schmidt number (S_c), Suction number(S) and Dufour number(D_u)have been discussed graphically. The numerical solutions of the above mentioned quantities for those parameters are computed and the obtained values are plotted graphically in Figures 18-32. For numerical solution implicitly, the shear stress(τ), Nusselt number$(N_u)$and Shearwood number(S_h)vursesτ have been illustrated in Figures 18-32. The profiles of shear stress(τ_x) for different parameters are shown in Figures 18-26. It is observed that, shear stress(τ_x)decreases with the increase of Visco-elastic parameter(α). It is observed that shear stress(τ_x)decreases with the decrease of Dufour number (D_u). Shear stress(τ_x)increased with the increase of (G_m)which has been shown in Figure 20. It is observed that shear stress(τ_x)increases with the increase of Grashof number(G_r)in Figure 21. Shear stress (τ_x)increases with the increase of Hartmann number(M_{ha})in Figure 22. Shearstress(τ_x)decreases with the increase of Prandtl number(P_r). Shear stress(τ_x)decreases with the increase of Suction number(S), Schimidt number(S_c)respectively. Shear stress(τ_x) increases with the increase of Soret number(S_r). Figure 26 shows that$\tau_x$decreases with the increase ofP_r. The profiles of Nusselt number for different parameters have been shown in Figures 27-29. It is observed that Nusselt number increases with the decrease of Dufour number(D_u), Nusselt number increases with the increase of Prandtl number$(P_r)$and Nusselt number increases with the increase of Suction number(S).A negligible effect of other

parameters figures are not discussed briefly. Other effects are not discussed in graphically for minor effects of parameters.

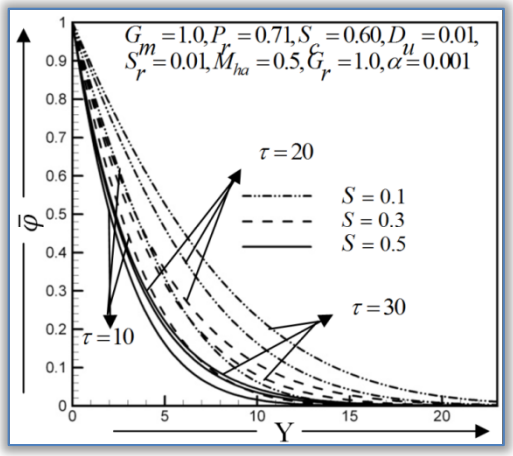

Figure 15. Concentration distributions $\bar{\varphi}$ for different values of Suction number, S.

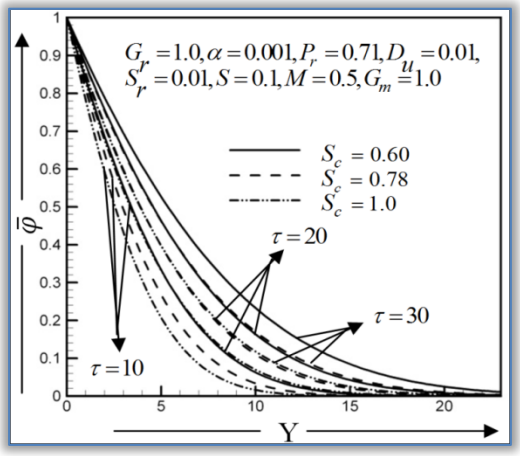

Figure 16. Concentration distributions $\bar{\varphi}$ for different values of Schmidt number, S_c.

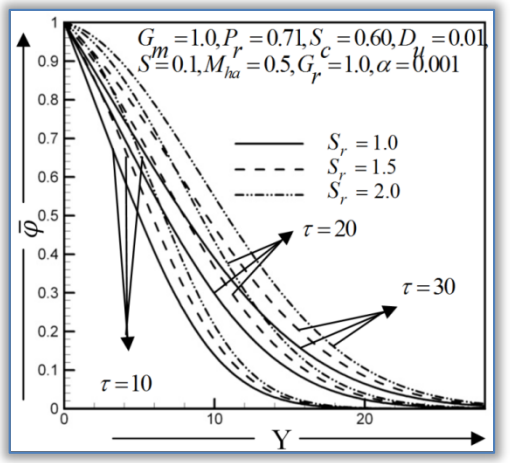

Figure 17. Concentration profiles φ for different values of Soret number, S_r.

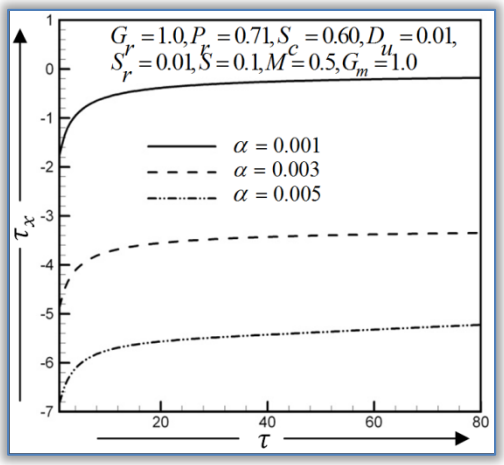

Figure 18. Shear stress τ_x for different values of visco-elastic parameter, α.

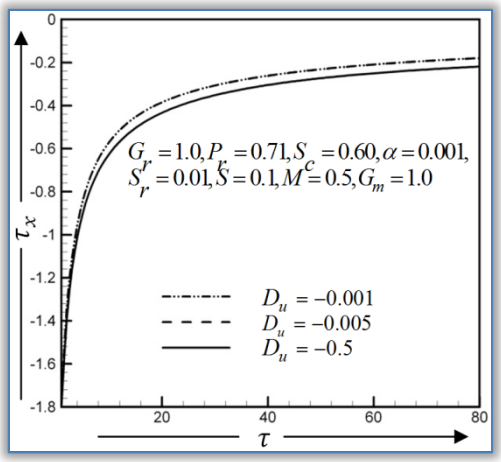

Figure 19. Shear stress τ_x for different values of Dufour number, D_u.

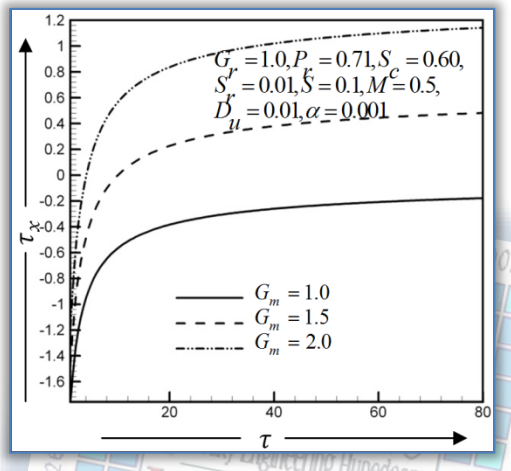

Figure 20. Shear stress τ_x for different values ofmodified Grashof number, G_m.

The curves of Shearwood number are presented in Figures 30-32. It is observed that the Sherwood number (S_h) increases with the increase of Suction number (S), the Sherwood number (S_h) increases with the increase of Schmidt number (S_c). The Sherwood number (S_h) decreases with the increase of Soret number (S_r) and the Sherwood number remains unchanged for other parameters.

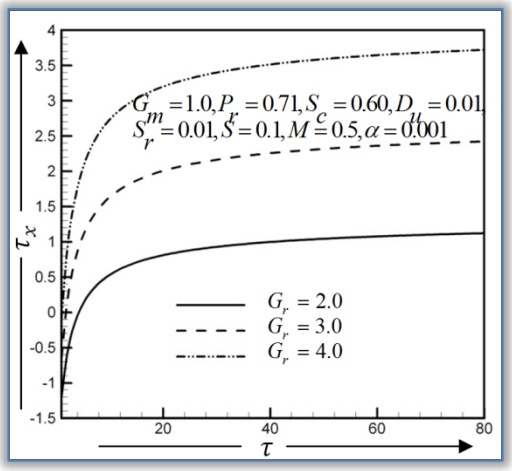

Figure 21. Shear stress τ_x for different values of Grashof number, G_r.

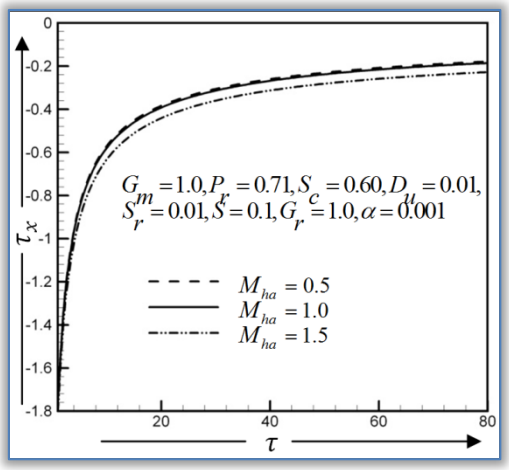

Figure 22. Shear stress τ_x for different values of Hartmann number, M_{ha}.

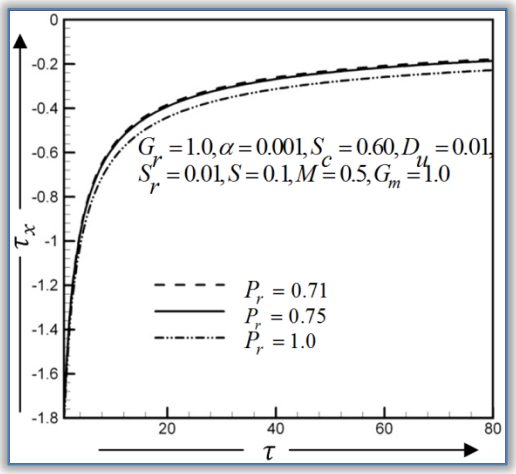

Figure 23. Shear stress τ_x for different values of prandtl number, P_r.

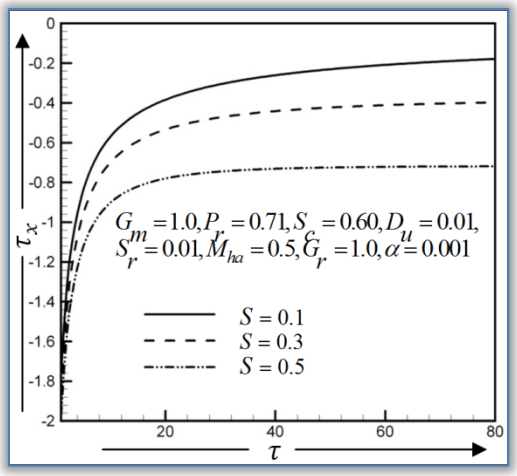

Figure 24. Shear stress τ_x for different values of Suction number, S.

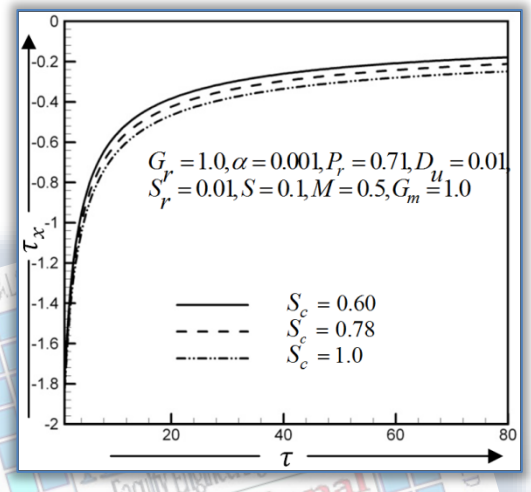

Figure 25. Shear stress τ_x for different values of Schmidt number, S_c.

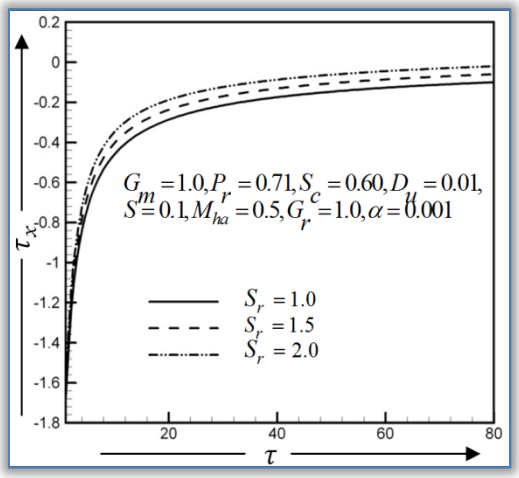

Figure 26. Shear stress τ_L for different values of Soret number, S_r.

Finally, a qualitative comparison of the present steady-state results with the published results (Gbadeyan et al. (2011)) is presented in table 1. The accuracy of the present results is qualitatively good in case of all the flow parameters.

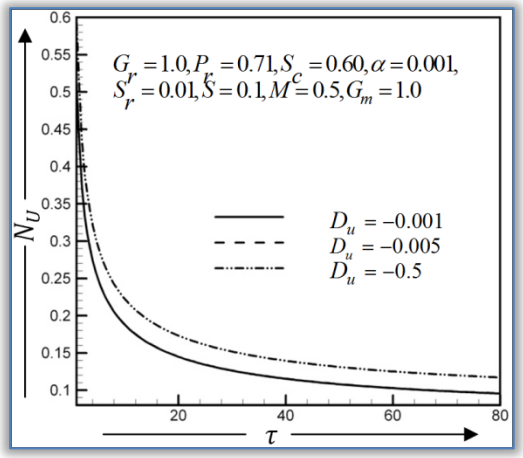

Figure 27. Nusselt number N_u for different values of Dufour number, D_u.

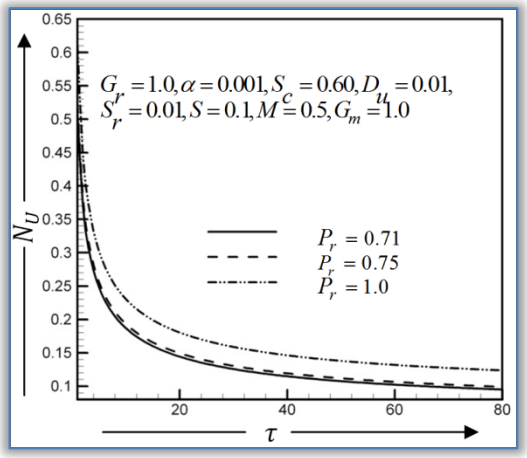

Figure 28. Nusselt number N_u for different values of Prandtl number, P_r.

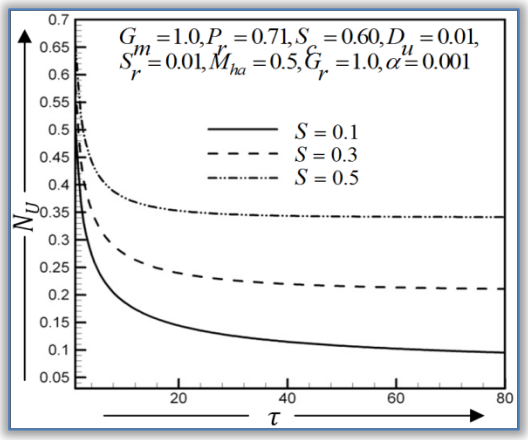

Figure 29. Nusselt number N_u for different values of Soret number, S.

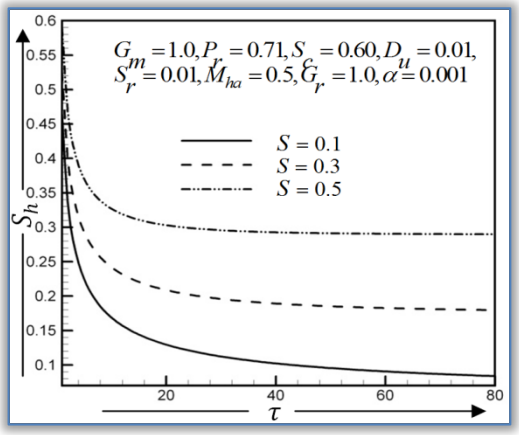

Figure 30. Sherwood number S_h for different values of Suction number,S.

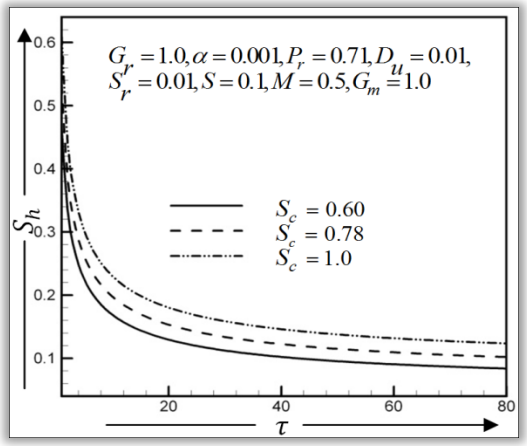

Figure 31. Sherwood number S_h for different values of Suction number, S_c.

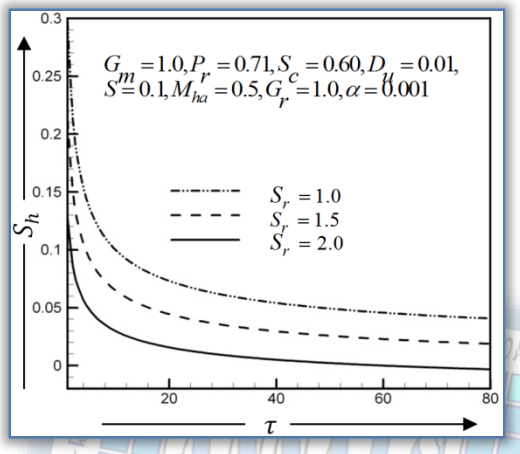

Figure 32. Sherwood number S_h for different values of Soret number, S_r.

Table 1. Qualitative comparison of the present results with the previous results

Increased Parameter	Previous results given by Gbadeyan et. al. (2011)			Present results					
	u	θ	ϕ	U	θ	$\overline{\varphi}$	τ_x	N_u	S_h
D_u	Inc.	Inc.		Inc.	Inc.		Inc.	Dec.	
M_{ha}	Dec.			Dec.			Dec.		
P_r		Dec.		Dec.	Dec.		Dec.	Inc.	
S_c				Dec.		Dec.	Dec.		Inc.
S_r			Inc.	Inc.		Inc.	Inc.		Dec.
α	Inc.	Dec.	Dec.	Dec.			Dec.		
S	Inc.	Dec.	Dec.	Dec.	Dec.	Dec.	Dec.	Inc.	Inc.

7. CONCLUSION

The effects of different parameters on velocity, temperature and concentration distributions, shear stress, Nusselt number and Sherwood number have been discussed graphically. The comparison between this solutions for parameters, has been presented graphically for velocity profiles, temperature distributions, concentration distributions, shear stress, Nusselt number and Sherwood number with published paper Gbadeyan et al. (2011). Form the comparison it has been found that the two solutions are qualitatively similar but not quantitatively similar and represents the same trend (increase or decrease).

(1) The velocity profiles decreases with the increase of $\alpha, M_{ha}, P_r, S_c, S$ while the velocity profiles increases with the increase of G_m, G_r, S_r .
(2) The velocity profiles decreases with the decrease of D_u.
(3) The Temperature distributions decreases with the decrease of D_u, while the Temperature distributions decreases with the increase of P_r.
(4) The Temperature distributions decreases with the increase of S, while the concentration distributions decreases with the increase of S.
(5) The concentration distributions decreases with the increase of S_c, while the concentration distributions increases with the increase of S_r.
(6) Shear stress (τ_x) decreases with the increase of α, P_r, S, S_c and decreases with the decrease of D_u , while shear stress increases with the increase of G_m, G_r, M_{ha}, S_r.
(7) Nusselt number (N_u) increases with the increase of P_r, S, while Nusselt number (N_u) increases with the decrease of D_u .
(8) Sherwood number (S_h) increases with the increase of S_c, S, while Sherwood number (S_h) decreases with the increase of S_r .

In this analysis, the effects of different parameters on the velocity, temperature distributions and concentration distributions have been discussed graphically. All the parameters, visco-elastic terms, thermal diffusion and mass diffusion terms are the main objective for this work, which has attracted the interest of any investigators in view of its important applications.

REFERENCES

[1.] Brinkman, H. C. (1947), "A Circulation of Viscous Force Extended by Flowing Fluid in a Dence Swarm of Particles", Appl. Sci. Res, vol. A(1), pp. 27-34.
[2.] Chaudhary, R. C. and Sharma, B. K. (2006), "Combined heat and mass transfer by laminar mixed convection flow from a vertical surface with induced magnetic field", J. Appl. Phys., vol. 99(3), pp. 034901.
[3.] Chowdhury, M. K. and Islam, M. N. (2000). "MHD free convection flow of visco-elastic fluid past an infinite vertical porous plate", Heat and Mass Transfer, vol. 36, pp. 439.
[4.] Das, S. S. Sahoo, S. K. and Dash, G. C. (2006), "Numerical Solution of Mass Transfer Effects on Unsteady Flow Past an Accelerated Vertical Porous Plate with Suction", Bulletin of Malysie. Math. Sci. Soc., vol. 29(1), pp. 33-42.
[5.] Gbadeyan, J. A., Idowu, A. S., Ogunsola, A. W., Agboola, O. O. and Olanrewaju, P.O. (2011), "Heat and mass transfer for Soret and Dufour's effect on mixed convection boundary layer flow over a stretching vertical surface in a porous medium filled with a viscoelastic fluid in the presence of magnetic field", Global Journal of Science Frontier Research, vol. 11(8), pp. 97-114.
[6.] Hayat, T., Mustafa, M, and Pop, I. (2010). "Heat and mass transfer for Soret and Dufour's effect on mixed convection boundary layer flow over a stretching vertical surface in a porous medium filled with a viscoelastic fluid" Communications in Nonlinear Science and Numerical Simulation, 15(9), pp. 1183-1196.
[7.] Mahanta, M. and Choudhury, R. (2012), "Mixed convective mhd flow of visco-elastic fluid Past a vertical infinite plate with mass transfer", International Journal of Scientific & Engineering Research, 3(2), pp. 1-7.
[8.] Nanousis, N. (1992), Astrophys. Space. Sci., vol. 191, pp. 313.
[9.] Nanousis, N. (1992). "Unsteady magnetohydrodynamic flows in a rotating elasto-viscous fluid" Astrophysics and Space Science, vol. 199(2), pp. 317-321.
[10.] Rajesh, V., (2011). "Heat source and mass transfer effects on mhd flow of an elasto-viscous fluid through a porous medium", International Journal of Engineering, vol. 2, pp. 205-212.
[11.] Rakesh, K., Khem, C., (2011), "Effect of Slip Conditions and Hall Current on Unsteady MHD Flow of a Viscoelastic fluid past an infinite Vertical porous plate through Pporous medium", International Journal of Engineering Science and Technology, vol. 3(4), pp. 3124-3133.
[12.] Samria, N. K., Prasad, R. and Reddy, M. U. S. (1990). "MHD free convection flow of an elasto-viscous fluid past an infinite vertical plate", Astro Physics and Space Science, vol.181, pp. 125-134.
[13.] Soundalgekar, V. M. and Puri, P. (1969). "On Fluctuating Flow of an Elastico-Viscous Fluid Past an Infinite Plate with Variable Suction", J. Fluid Mechanics, vol. 35(3), pp. 561-573.